Aquatic Toxicology 262 (2023) 106662

Contents lists available at ScienceDirect

Aquatic Toxicology

journal homepage: www.elsevier.com/locate/aqtox

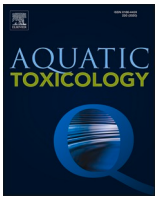

Acute bioaccumulation and chronic toxicity of olivine in the marine amphipod *Gammarus locusta*

Gunter Flipkens [a,*], Katharina Horoba [a], Kobe Bostyn [a], Luna J.J. Geerts [b], Raewyn M. Town [a], Ronny Blust [a]

[a] ECOSPHERE, Department of Biology, University of Antwerp, Groenenborgerlaan 171, 2020, Antwerp, Belgium
[b] Geobiology, Department of Biology, University of Antwerp, Universiteitsplein 1, 2610, Antwerp, Belgium

ARTICLE INFO

Keywords:
Olivine
Ocean alkalinization
Nickel
Chromium
Enhanced silicate weathering
Marine ecotoxicology

ABSTRACT

Active atmospheric carbon dioxide removal (CDR) is needed at a gigaton scale in the next decades to keep global warming below 1.5 °C. Coastal enhanced silicate weathering (CESW) aims to increase natural ocean carbon sequestration via chemical weathering of finely ground olivine ($Mg_xFe_{(1-x)}SiO_4$) rich rock dispersed in dynamic coastal environments. However, the environmental safety of the technique remains in question due to the high Ni and Cr content of olivine. Therefore, we investigated the short term bioaccumulation and chronic toxicity of olivine in the marine amphipod *Gammarus locusta*. Acute 24-h olivine exposure resulted in significant grain size dependent olivine ingestion and subsequent Ni and Cr accumulation in tissues. Thousands of small (mainly ≤ 10 μm) olivine grains were ingested by *G. locusta*, but their importance for trace metal bioaccumulation requires additional research. Most olivine grains were egested within 24 h. Chronic 35-day olivine (3–99 μm) exposure reduced amphipod survival, growth, and reproduction, likely as a result of metal induced oxidative stress and disturbance of major cation homeostasis. Amphipod reproduction was significantly reduced at olivine concentrations of 10% w/w and higher. In the context of ecological risk assessment, application of an arbitrary assessment factor of 100 to the highest no observed effect concentration of 1% w/w olivine yields a very low predicted no-effect concentration (PNEC) of 0.01% w/w olivine. This low PNEC value highlights the urgent need for additional marine olivine toxicity data to accurately assess the environmentally safe scale of coastal enhanced weathering for climate change mitigation.

1. Introduction

Limiting global warming to 1.5 °C requires gigaton scale atmospheric carbon dioxide (CO_2) removal (CDR) in the next decades (Minx et al., 2018). Ocean alkalinization (OA) via coastal enhanced silicate weathering (CESW) has been proposed as a scalable CDR strategy to help stabilize global temperatures and minimize adverse effects on natural ecosystems and human societies (Meysman and Montserrat, 2017). This technique aims to accelerate natural chemical weathering of silicate minerals by distributing suitable finely ground source rock in dynamic coastal areas. During silicate mineral dissolution, total alkalinity in seawater increases via the consumption of protons, which drives atmospheric CO_2 drawdown (Meysman and Montserrat, 2017). The relatively fast weathering kinetics (Rimstidt et al., 2012) and abundance (Caserini et al., 2022) of olivine ($Mg_xFe_{(1-x)}SiO_4$) rich rock (i.e. dunite) make it an attractive option for CESW. Possible co-benefits of CESW include counteracting ocean acidification and enhanced primary production of silicifiers (e.g. diatoms) via proton consumption and supply of iron (Fe) and silicon (Si), respectively (Bach et al., 2019). In contrast to these benefits, coastal enhanced olivine weathering could have adverse ecosystem impacts as a result of both geophysical environmental changes (e.g. sediment siltation and pore space clogging) (Schlacher et al., 2012) and nickel (Ni) and chromium (Cr) accumulation to potentially toxic levels (Flipkens et al., 2021).

A recent modelling study showed that relatively low olivine applications (0.059–1.4 kg m^{-2} seabed) could potentially lead to sediment Ni concentrations that exceed existing environmental quality standards and pose a toxicological threat to benthic marine biota (Flipkens et al., 2021). Furthermore, smaller olivine particles could potentially be more toxic than larger ones due to their faster weathering rate and easier ingestion by various marine organisms (Duan et al., 2022). However, due to the paucity of data on olivine exposure effects on aquatic biota,

* Corresponding author.
E-mail address: Gunter.Flipkens@uantwerpen.be (G. Flipkens).

https://doi.org/10.1016/j.aquatox.2023.106662
Received 12 June 2023; Received in revised form 31 July 2023; Accepted 13 August 2023
Available online 14 August 2023

currently limited to microorganisms (Hutchins et al., 2023; Ren et al., 2021; Xie et al., 2023), accurate ecological risk assessment of coastal enhanced olivine weathering remains impossible.

Therefore, we investigated the acute 24 to 96 h bioaccumulation and chronic 35-day toxicity of olivine in the benthic marine amphipod *Gammarus locusta*. This species has been reported as the most sensitive European marine *Gammarus* spp. to environmental disturbance (e.g. hypoxia and temperature fluctuations) and contaminant exposure (e.g. oil spills and trace metals) (Costa and Costa, 2000), making it a suitable test species to examine olivine bioaccumulation and toxicity. Based on the ingestion of 500 × 20 μm polyamide fibers by the freshwater *Gammarus fossarum* we hypothesized that olivine grains of comparable dimensions or smaller could be ingested (Blarer and Burkhardt-Holm, 2016). Furthermore, we expected olivine dose and grain size dependent metal accumulation and toxic effects (Duan et al., 2022; Flipkens et al., 2021). Finally, we hypothesized lower bioavailability of Cr compared to Ni due to the low aqueous solubility of chromite, which is the dominant Cr-bearing phase in dunite rock (Flipkens et al., 2021).

2. Material and methods

2.1. Amphipod collection and housing

Amphipods were collected from the relatively uncontaminated Eastern Scheldt estuary (51°27′31.6″N 4°04′50.4″E, Krabbendijke, the Netherlands) during low tide where they were abundantly present on sea lettuce (*Ulva* sp.) (den Otter et al., 2023). Amphipods were microscopically identified as *G. locusta* in the laboratory (Supplementary Section S1). Amphipods were cultured and experiments were conducted under controlled temperature (experiment specific) and light conditions (12:12 h light:dark cycle). Amphipods were housed in a 210 L polyethylene tank filled with artificial seawater (ASW), a 1 cm layer of control sediment (see Section 2.2.) and stones from the sampling location. To prepare ASW, seasalt (hw-Marinemix®, 35.75 g L^{-1}) was added to ultrapure water (Eurowater DPRO B1 – 1/1) and aerated for at least 24 h. Amphipods were fed *Ulva* sp. *ad libitum* and commercial fish food (Sera Micron Nature, 1 mg amphipod^{-1}) three times per week (Neuparth et al., 2002). A protein skimmer and trickling filter were installed, and weekly 15 to 30% water changes were conducted. Before water renewal, nitrogenous waste concentrations were measured with commercial test kits (Tetra) and seawater temperature, pH, dissolved oxygen (DO) and conductivity were measured with a HQ30D portable multimeter (Hach). The conductivity cell and pH electrode were calibrated before each use with NIST conductivity standards (12880 μS cm^{-1} and 50,000 μS cm^{-1}, VWR international) and pH buffers (pH 4.00, 7.00, and 10.01, VWR international), respectively. The pH of a TRIS (2-amino-2-hydroxy-1,3-propanediol) and AMP (2-aminopyridine) buffer were measured to calibrate pH measurements to the appropriate total pH scale for seawater (Dickson et al., 2007).

2.2. Sediment collection and geochemical analyses

Surficial (<10 cm depth) control sediment was collected with a shovel at the amphipod collection site. In the laboratory, sediment was wet sieved through a 500 μm screen to remove macrofauna before storage in a clean HDPE bucket at 4 °C until experimental use. VANGUARD refractory grade dunite sand from Åheim (Norway) was obtained from Sibelco. This sand is composed of 69 to 86 wt.% olivine, of which 93.2–93.4% is forsterite and 6.6–6.8% is fayalite (characterization procedure in Supplementary Section SI 2) and will be referred to as olivine throughout the text.

For sediment characterization, organic matter (SOM) content was determined via loss on ignition according to protocol by Heiri et al. (2001). Grain size distribution was analysed with a laser diffraction particle analyzer (Mastersizer 2000, Malvern Panalytical) according to standard operating procedures without chemical pre-treatment. Different sizes of olivine sand will be referred to by their volume-based effective grain size D10 and D90 throughout the text (e.g. 3–99 μm olivine). Finally, the elemental composition was determined via ICP-OES (iCAP 6300 Duo, Thermo Scientific) after microwave-assisted acid digestion following a modified chromite ore digestion protocol that is provided in Supplementary Section SI 2 (CEM Corporation, 1999).

2.3. Acute exposure to different olivine sizes

2.3.1. Experimental set-up

For the accumulation phase, adult amphipods (metasomatic length (ML) = 9–17 mm) were individually exposed for 24 h in high-density polyethylene (HDPE) beakers filled with 400 mL ASW and 25 ± 0.03 g (~4 mm layer) of different olivine grain sizes (3–99 μm, 93–332 μm, and 208–488 μm) (Fig. 1A). Beakers were randomly assigned to treatments and rinsed with 2% V/V HCl and ultrapure water before use. Seven replicate beakers, each comprising one individual (overall total of 3 males and 4 females or vice versa) were set up for each olivine treatment and an ASW control (400 mL ASW) and continuously aerated with aeration lines fitted with plastic tips positioned 6 cm above the sediment. Olivine was allowed to settle for 24 h and amphipods were starved for 24 h prior to exposure. Amphipods were photographed on 1 mm graph paper for sex and ML determination. The ML is the distance between the anterior end of the rostrum and the posterior end of the last metasomatic segment and was measured in ImageJ using the segmented line tool (Supplementary Fig. A.2). A clear difference in gnathopod morphology allowed sex identification of adult *G. locusta* (Supplementary Fig. A.3). For the depuration phase, adult amphipods exposed to different olivine grain sizes for 24 h (as described above) were rinsed with ASW and transferred to clean HDPE beakers filled with 400 mL ASW (Fig. 1A). Depuration lasted 24 h with 7 experimental replicates (3 males and 4 females or vice versa) (Fig. 1A). Amphipods were collected at the end of the accumulation and depuration phase for metal analysis as described in Section 2.3.2.

Seawater temperature (17.5 ± 0.6 °C), salinity (33 ± 0.4‰), pH (8.1 ± 0.06), dissolved oxygen (7.7 ± 0.1 mg L^{-1}), and nitrogenous waste concentrations (NO_3^- = 12.5 mg L^{-1}, NO_2^- ≤ 0.3 mg L^{-1}, NH_3/NH_4^+ = 0.25 mg L^{-1}) were measured in fresh ASW and experimental beakers after the 24 h exposure and 24 h depuration (individual values provided in Supplementary Section SI 3.1). Simultaneously, 0.2 μm filtered (Chromafil XTRA PES-20/25, Macherey-Nagel) seawater samples were collected for dissolved metal analysis. After collection, samples were diluted 20 times with 2% V/V TraceMetal™ Grade nitric acid (Fisher Scientific) to minimize matrix effects during analysis via HR-ICP-MS (Element XR, Thermo Fisher Scientific). Procedural blanks (2% V/V HNO_3) and certified reference material (1643f, NIST) was measured for quality control.

2.3.2. Amphipod elemental analysis

Amphipods collected for whole body element analysis were rinsed with ultrapure water and dried in preweighed 5 mL tubes at 60 °C for 48 h. Standard reference material (SRM-2976 mussel tissue, NIST) and procedural blanks (empty 5 ml tubes) were included for quality control. Sample dry weight was measured with an ultra-microbalance (Sartorius SE2). Subsequently, 400 μL of concentrated (67–69%) TraceMetal™ Grade nitric acid (Fisher Scientific) was added to the samples to digest at room temperature for at least 12 h. Next, the samples were heated at 105 °C for 15 min in an SC154 HotBlock® (Environmental Express). Subsequently, 50 μL of 30–32% W/W H_2O_2 (Fisher Scientific) was added and samples were incubated at room temperature for 10 min before additional heating at 105 °C for 15 min. After digestion, samples were diluted to 2.2% V/V HNO_3 with ultrapure water before elemental analysis via HR-ICP-MS. Certified reference material (1643f, NIST) was included for analytical quality control. In the different experiments (N =

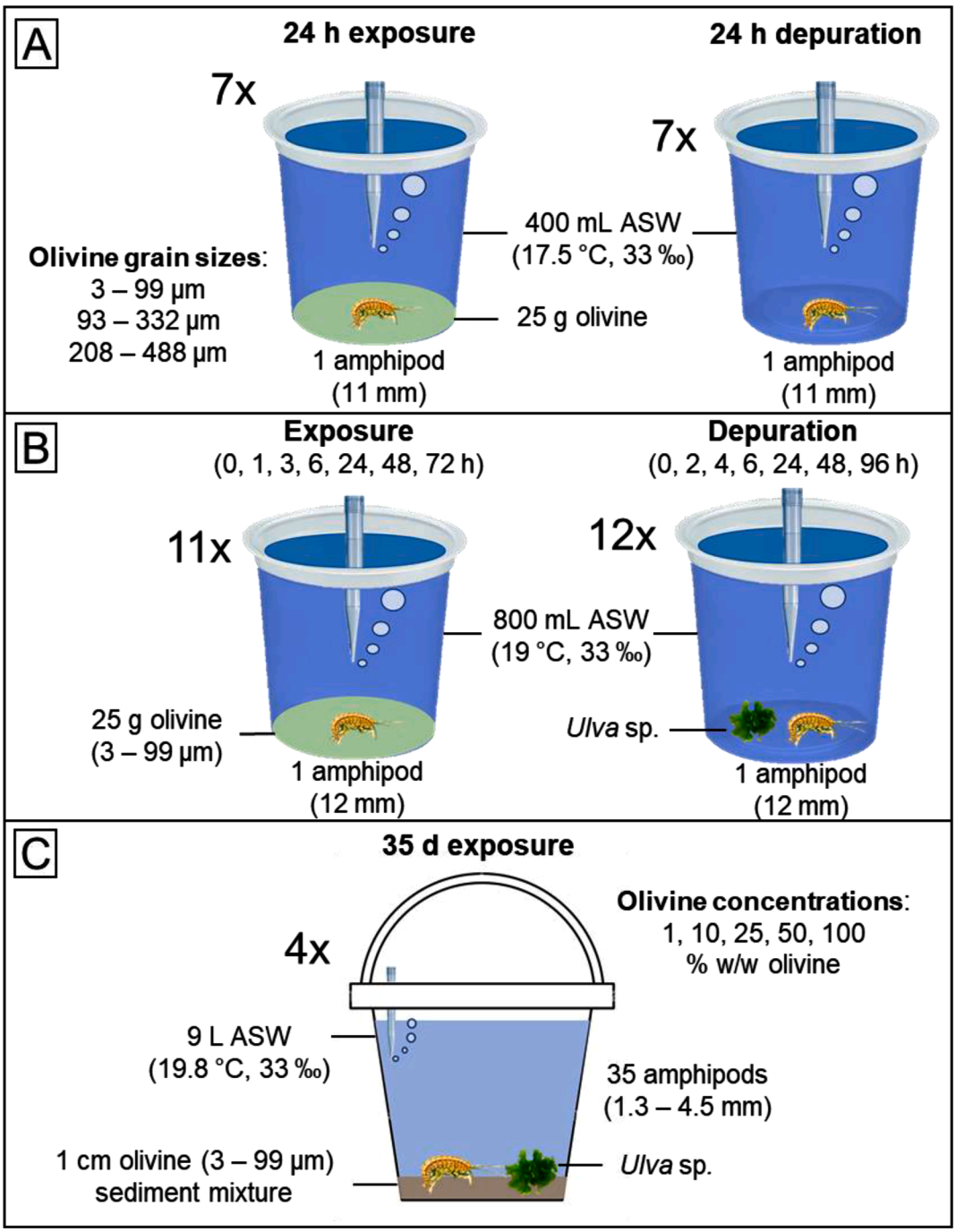

Fig. 1. Schematic representation of the (A) acute grain size experiment, (B) uptake and elimination experiment and (C) chronic toxicity test are shown. ASW = artificial seawater.

3) average element recoveries for the SRM-2976 ranged between 60 and 85% for Ni and 20 to 66% for Cr.

2.4. Acute 3–99 µm olivine uptake and elimination

2.4.1. Experimental set-up

For the accumulation phase, clean HDPE beakers were filled with 25 g (~2 mm layer) of dry 3–99 µm olivine and 800 mL ASW (Fig. 1B). Beakers were randomly assigned to treatments and continuously aerated as described previously. Olivine was allowed to settle and adult amphipods were not fed for 24 h before exposure. Adult amphipods (ML = 8–16 mm) were photographed before exposure for length and sex determination as described previously. During the accumulation phase, amphipods were not fed and exposed to 3–99 µm olivine for 0, 1, 3, 6, 24, 48, and 72 h with 11 replicate beakers, each comprising one individual (7 males and 4 females) per exposure time (Fig. 1B). for the depuration phase, adult amphipods were exposed to olivine for 72 h as described above and subsequently transferred to clean HDPE beakers with 800 mL ASW and 100 mg *Ulva* sp. (Fig. 1B). Before transfer, amphipods were rinsed with ASW. Depuration lasted 0, 2, 4, 6, 24, 48, or 96 h with 12 replicate beakers, each comprising one individual (7 males and 5 females) for each depuration period (Fig. 1B). *Ulva* sp. was provided *ad libitum* during the depuration phase.

Seawater temperature (19.1 ± 0.4 °C) and pH (8.2 ± 0.2) were measured at each sampling time during the accumulation and depuration experiment (Supplementary Fig. A.6). Furthermore, amphipod

survival was monitored and samples for dissolved metal analysis were collected. Seawater salinity (33 ± 0.8‰), dissolved oxygen (7.5 ± 0.1 mg L^{-1}) and concentrations of nitrate (≤12.5 mg L^{-1}), nitrite (<0.3 mg L^{-1}) and ammonium (≤0.25 mg L^{-1}) were measured at the start and end of the experiment in at least three replicates (Supplementary Fig. A.6). Surviving amphipods were sampled at each timepoint to determine whole body metal accumulation (6 to 8 individuals) and ingested olivine grain sizes (1 to 3 individuals). Temporal differences in the ingested olivine grain size distribution were not investigated due to limited amount of samples per timepoint.

2.4.2. Ingested olivine size analysis

Amphipods collected for ingested olivine size analysis were rinsed with ultrapure water, euthanized with 70% V/V ethanol, and dissected under a stereomicroscope to collect ingested olivine particles. Then, olivine samples were washed with ultrapure water and dried at 60 °C for 12 h. Afterwards, dry olivine grains were mounted on aluminium pin stubs with double sided carbon tape for imaging at 1600× magnification with a Phenom ProX scanning electron microscope (SEM). The particle size distribution was determined in ImageJ. First, the image was calibrated using the SEM image scale. Afterwards, a Gaussian blur (sigma = 1.5) was applied and the image was thresholded (default option, Auto threshold). Then, touching particles were separated using the watershed algorithm for irregular features (erosion cycle number = 12) before analysis using the "Analyze Particles" command. Particles on the edge of the image were excluded and interior holes in grains were filled. Finally, the Feret's diameter and equivalent sphere diameter were derived for comparison to laser diffraction data.

2.5. Chronic 3–99 μm olivine toxicity test

2.5.1. Experimental set-up

A chronic 35-day olivine toxicity test was conducted according to the study by Neuparth et al. (2005) with minor modifications. Twenty-four clean HDPE buckets were filled with a 1 cm layer of wet control sediment manually mixed with different concentrations of dry 3–99 μm olivine (0, 1, 10, 25, 50, or 100% dry w/w, Supplementary Section 5.1). Four replicates were used for each olivine treatment and the sediment control. Subsequently, samples for geochemical analysis (Section 2.2.) were collected and 5 small stones (~8 cm^3 in size) were added to provide shelter. Buckets were slowly filled with 8 L of ASW and aerated as described previously. The sediment was left to equilibrate for 7 days before amphipod addition.

The chronic bioassay started when 1 g of *Ulva* sp. and 35 juvenile amphipods (ML = 1.3–4.5 mm) were carefully added to the experimental buckets with a Pasteur pipette. Amphipod survival and food availability were checked daily. *Ulva* sp. was provided *ad libitum* in portions of 1 g and commercial fish food (Sera Micron Nature, 0.5 mg amphipod^{-1}) was provided once a week. Seawater temperature (19.8 ± 0.4 °C), pH (8.10 ± 0.06), DO (7.1 ± 0.1 mg L^{-1}), salinity (33 ± 0.5‰), and nitrogenous waste concentrations (NO_3^- ≤ 12.5 mg L^{-1}, NO_2^- ≤ 0.3 mg L^{-1}, NH_3/NH_4^+ ≤ 0.25 mg L^{-1}) were measured twice a week before conducting a 50% water renewal (Supplementary Fig. A.8). Furthermore, seawater samples for dissolved metal and dissolved organic carbon (DOC) analysis were collected once a week before and after water change. Additionally, seawater total alkalinity (TA) was measured on day 14 and 35. Methods and results of DOC and TA analysis are provided in Supplementary Section SI 5.2.

At the end of the experiment, the contents of the buckets was sieved through 1000 and 250 μm mesh sieves to collect surviving adults and juveniles, respectively. The juveniles were counted and all adult amphipods were photographed on 1 mm graph paper for size and sex determination. Afterwards, adult males and non-gravid females were rinsed with ultrapure water and pooled (1–4 pools) for metal analysis (4–13 individuals, 28–166 mg w.w.) and thiobarbituric acid reactive substances (TBARS) determination (3–6 individuals, 45–171 mg w.w.). Pooled amphipods for TBARS measurements were immediately frozen in liquid nitrogen and stored at −80 °C until analysis. Gravid females were preserved in 70% V/V ethanol (VWR International) at 4 °C to study reproductive endpoints within a week.

2.5.2. Biological endpoints

Several biological endpoints were determined at the end of the 35-day experiment, including amphipod survival, sex ratio, growth, reproductive traits, whole body trace metal and major cation concentrations, and lipid peroxidation. The sex ratio was determined by dividing the number of surviving males by the number of surviving females for each replicate. The individual growth was determined as the ML of the surviving amphipods. The number of gravid females was divided by the total number of females in each replicate to derive the percentage gravid females. The number of juveniles and embryos in the brood pouch of gravid females was counted to determine the total juvenile and embryo production. Whole body metal (Ni, Cr, Fe, Cu, Zn, Cd, Mn) and major cation (Na, K, Ca, Mg) concentrations were measured for pooled amphipods of each replicate as described previously (Section 2.3.2). The TBARS content was quantified using a thiobarbituric acid reactive substances (TBARS) assay (Cayman Chemical) following the manufacturer's guidelines for tissue homogenates. The TBARS levels were determined spectrophotometrically at a wavelength of 530 nm with a multimode microplate reader (Spark, Tecan). TBARS concentrations were calculated from an malondialdehyde (MDA) colorimetric standard curve and expressed per gram of sample wet weight (μmol TBARS g^{-1} w.w.).

2.6. Statistical analyses

Kruskal–Wallis analysis of variance (ANOVA) was performed on data of the acute experiments to investigate differences in metal accumulation between olivine treatments and timepoints. A non-parametric test was conducted since model residuals were not normally distributed according to QQ plots and Shapiro-Wilk tests. Homoscedasticity of model residuals was assessed via residual plots and Levene's tests. Relevant post hoc pairwise comparisons were made using Dunn's test with "holm" p value adjustment method.

One-way ANOVA and Dunnett's Tests were conducted to investigate differences in amphipod survival, reproduction, trace metal accumulation and major ion concentrations between treatments and the control after 35-day exposure. Model assumptions were assessed and non-parametric tests were conducted if model residuals were not normally distributed as described in the previous paragraph. Robust standard errors were used to correct for unequal residual variance (i.e. heteroscedasticity) using the vcov=``sandwich'' argument from the 'sandwich' package. A linear mixed effects model (lmerTest package) was fit to investigate the effect of chronic olivine exposure on amphipod growth. Bucket ID was included as a random effects term and nested in treatment. T-tests using the Satterthwaite's method were performed to investigate differences between treatments and the control.

The relationship between experimental endpoints and whole body Ni concentrations was assessed via simple linear regressions and Kendall correlation coefficients to investigate if adverse effects could be empirically linked to metal toxicity. Kendall rank-based correlation tests were used since data were not normally distributed according to QQ plots and Shapiro-Wilk tests. Whole body Cr concentrations were not included in the linear regressions due to multicollinearity issues. Diagnostic plots were constructed to assess model assumptions. If needed, the whole body Ni concentrations were log transformed to improve linearity of the model residuals and robust linear regression was used to deal with influential outliers (Cook's distance >0.5). Results were considered statistically significant when p value <0.05. Statistical analyses were conducted in RStudio (version 2022.12.0 + 353) using R version 4.2.1 and figures were constructed in GraphPad Prism version 9.5.1 for

Windows.

3. Results and discussion

3.1. Sediment characteristics

The geochemical properties of Eastern Scheldt control sediment and olivine treatments are provided in Table 1. Overall, the average SOM content of control sediment (1%) and olivine (0.15–1.5%) were relatively low compared to the broad range of total organic carbon concentrations reported for estuarine sediments (0.3–23%) (Chakraborty et al., 2015; Ouyang et al., 2006). Average concentrations of Cr were 24 to 33 times higher in olivine (22–30 μmol g^{-1} d.w.) compared to control sediment (0.9 μmol g^{-1} d.w.), while average olivine Ni concentrations (36–41 μmol g^{-1} d.w.) were approximately 1000 times higher than control sediment (0.036 μmol g^{-1} d.w.). Additionally, significantly higher Mg and Fe concentrations are found in olivine (respectively 9043 and 652 μmol g^{-1} d.w.) compared to control sediment (respectively 80 and 85 μmol g^{-1} d.w.) (Supplementary Table A.2). However, low aqueous solubility of Fe, high background Mg concentrations in seawater, and essentiality of both elements infer that these metals are of low ecotoxicological concern compared to Ni and Cr (Meysman and Montserrat, 2017). Concentrations of Mg, Fe, Al, Mn, Co, and Zn in olivine and control sediment are provided in Supplementary Section SI 2.

3.2. Acute exposure to different olivine sizes

All amphipods survived the acute bioaccumulation experiment. However, olivine exposure resulted in a significant grain size dependent increase of whole body Ni and Cr concentrations (Fig. 2A and B). Median whole body Ni concentrations were significantly elevated in the 93–332 μm (0.55 μmol g^{-1} d.w., $p = 0.011$) and 3–99 μm (2.3 μmol g^{-1} d.w., $p < 0.001$) olivine treatments compared to the ASW control (0.13 μmol g^{-1} d.w.) after 24 h exposure (Fig. 2A). Median dissolved Ni concentrations were higher for smaller grain sizes and were significantly elevated ($p = 0.029$) in the 3–99 μm treatment (0.76 μmol L^{-1}) compared to the seawater control (0.050 μmol L^{-1}) (Fig. 2C). Higher dissolved Ni for smaller olivine grain sizes can be explained by the larger reactive olivine surface area, which enhances olivine dissolution and trace metal release (Rimstidt et al., 2012). After 24 h depuration, median Ni concentrations remained significantly elevated in amphipods exposed to 3–99 μm olivine (0.83 μmol g^{-1} d.w., $p = 0.0011$) compared to ASW control amphipods (0.10 μmol g^{-1} d.w.) (Fi. 2A). Dissolved Ni concentrations in ASW did not differ significantly between treatments (0.029–0.079 μmol L^{-1}, $N = 12$) at the end of the depuration phase (Fig. 2C).

Median whole body Cr concentrations were significantly elevated in all olivine treatments (median values of 0.098 to 0.39 μmol g^{-1} d.w.) compared to the ASW control (0.011 μmol g^{-1} d.w.) after 24 h exposure (Fig. 2B). The median Cr accumulation was 3 to 8 times lower than the median Ni accumulation (Fig. 2B), which can partly be explained by the 1.2 to 1.9 times lower Cr compared to Ni content of the experimental olivine (Table 1). Furthermore, dissolved Cr concentrations remained below the detection limit (0.38 nmol L^{-1}) in all treatments except the 3–99 μm olivine treatment (median = 0.048 μmol L^{-1}) (Fig. 2D). After 24 h depuration, the median Cr body burden was still significantly elevated in amphipods exposed to 3–99 μm olivine (94 nmol g^{-1} d.w., $p = 0.046$) compared to ASW control amphipods (0.015 nmol g^{-1} d.w.) (Fig. 2B) and dissolved Cr concentrations remained below the detection limit (Fig. 2D).

Limited Cr accumulation in ASW is likely explained by the low aqueous solubility of chromite ($FeCr_2O_4$), which is the dominant Cr-bearing phase in dunite rock (Flipkens et al., 2021). Hence, elevated whole body Cr concentrations can be mainly ascribed to olivine grains in the guts of exposed amphipods. Given the Cr content of the ingested olivine sizes (Fig. 4A), more than 450,000 olivine grains would have to be ingested (~3.6% of gut volume) to result in the Cr concentrations observed in the 3–99 μm olivine treatment (Fig. 2B) (Supplementary Section SI 3.3). Based on the potential dissolution rate of ingested olivine, a dietary Cr exposure rate of 0.17 nmol g^{-1} d.w. d^{-1} was derived (Supplementary Section SI 3.4), which was significantly lower than the estimated waterborne Cr uptake rate between 1.4 and 4.1 nmol g^{-1} d.w. d^{-1} (Wang et al., 1997). A similar conclusion can be drawn for Ni (Supplementary Section SI 3.4). However, after 24 h depuration median whole body Ni (0.83 μmol g^{-1} d.w.) and Cr (0.094 μmol g^{-1} d.w.) accumulations were approximately 28 and 20 to 59 (depending on the Cr oxidation state) times higher than expected assuming the calculated metal uptake rates. Uncertainties regarding the number of ingested grains, olivine dissolution rate, and waterborne metal uptake rate likely explain this discrepancy between observed and predicted Ni and Cr bioaccumulation. Hence, further research is required to assess the importance of olivine ingestion as a trace metal exposure pathway in marine biota.

Table 1
Geochemical properties of the experimental sediments. Sediment organic matter content (SOM, expressed in %), volumetric effective grain sizes (D, expressed in μm) and nickel (Ni) and chromium (Cr) concentrations (μmol g^{-1} d.w.) of control sediment and different olivine (ol) sizes. Data for the different 3–99 μm olivine concentrations (% w/w) of the chronic experiment are also provided. Mean ± S.D. values are shown ($N = 4$–5).

Sediment type	SOM (%)	D10 (μm)	D50 (μm)	D90 (μm)	Ni (μmol g^{-1} d.w.)	Cr (μmol g^{-1} d.w.)
Control	1.0 ± 0.04	71 ± 1	126 ± 3	222 ± 8	0.036 ± 0.018	0.90 ± 0.16
3–99 μm ol						
1% w/w	1.01 ± 0.03	69 ± 0.5	125 ± 0.8	220 ± 2	0.40[a]	1.2[a]
10% w/w	1.14 ± 0.03	33 ± 14	116 ± 3	217 ± 3	3.7[a]	3.8[a]
25% w/w	1.36 ± 0.03	12 ± 2	99 ± 2	206 ± 2	9.1[a]	8.1[a]
50% w/w	1.34 ± 0.04	5.8 ± 0.2	62 ± 3	175 ± 3	18[a]	15[a]
100% w/w	1.53 ± 0.19	3.23 ± 0.06	24 ± 0.2	99 ± 2	36 ± 2	30 ± 2
93–332 μm ol	0.29 ± 0.04	93 ± 7	189 ± 5	332 ± 5	38 ± 0.9	23 ± 0.9
208–488 μm ol	0.15 ± 0.04	208 ± 3	320 ± 5	488 ± 7	41 ± 0.4	22 ± 3

[a] Concentrations of Ni and Cr for the 1% w/w to 50% w/w 3–99 μm olivine were not analytically determined, but derived from the measured concentrations in the control sediment and 100% w/w 3–99 μm olivine.

3.3. Acute 3–99 μm olivine uptake and elimination

3.3.1. Trace metal accumulation and depuration

Most amphipods survived acute 72-h exposure to 3–99 μm olivine (93%) and depuration in ASW (88%). However, lethargic behaviour was observed after 24 h of exposure. Median amphipod whole body Ni concentrations rapidly increased upon olivine exposure and remained stable around 1.0 to 1.4 μmol g^{-1} d.w. after 24 hours of exposure (Fig. 3A). Median dissolved Ni concentrations were elevated at the start of the experiment (0.64 μmol L^{-1}) and further increased up to 1.0 μmol L^{-1} after 72 h as a result of olivine dissolution (Fig. 3C). Considerable variation in whole body trace metal accumulation was observed, likely due to differences in olivine ingestion among individuals.

Median whole body Ni concentrations decreased by approximately 60% from 1.0 to 0.42 μmol g^{-1} d.w. after 6 h of depuration which was still elevated compared to 0.033 μmol g^{-1} d.w. in unexposed amphipods (Fig. 3A). Afterwards, whole body Ni concentrations remained stable and varied little among individuals, suggesting that most olivine grains were egested within 24 hours (Fig. 3A). Olivine egestion was confirmed via microscopic examination, although some olivine grains were still

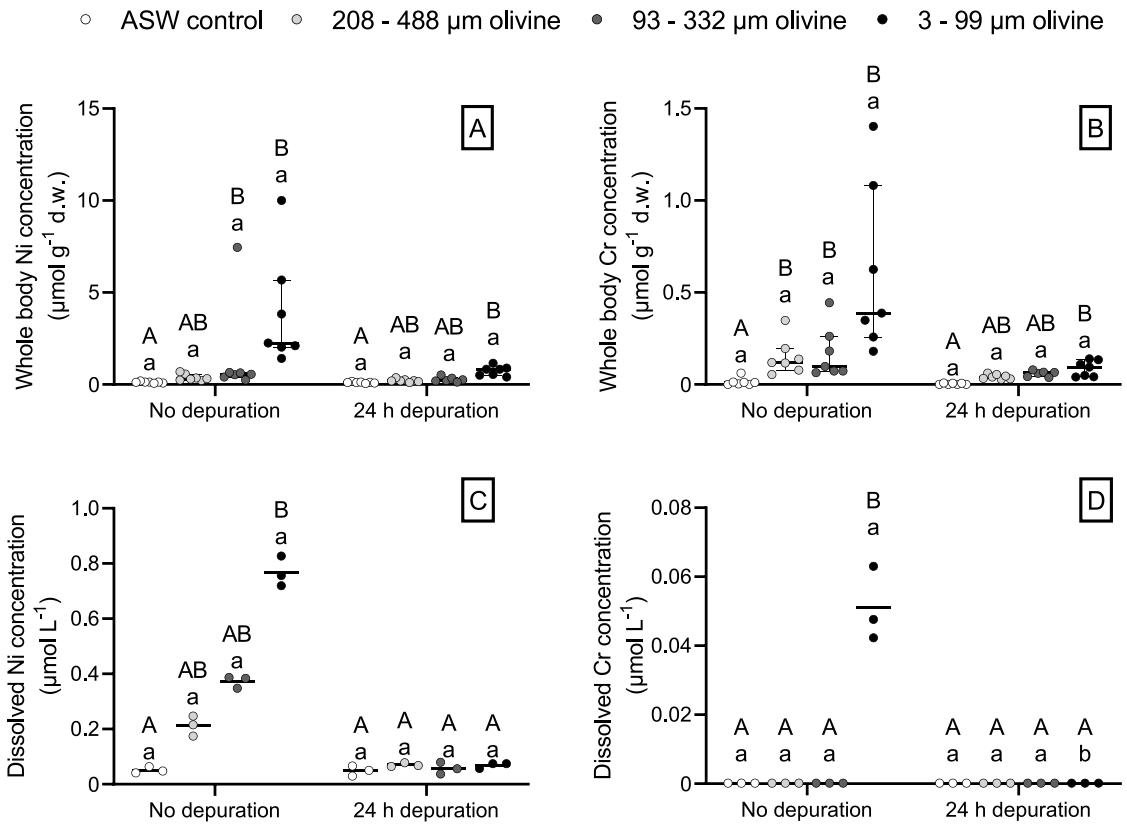

Fig. 2. Whole body concentration (µmol g^{-1} dry weight) of (A) nickel (Ni) and (B) chromium (Cr) in amphipods exposed to various olivine sizes for 24 h and subsequently not depurated or depurated for 24 h before analysis. Median and IQR are shown ($N = 6$ or 7). Dissolved concentrations (µmol L^{-1}) of (C) Ni and (D) Cr in artificial seawater at the end of the accumulation and depuration phase (Mean, $N = 3$). Lower case letters indicate significant differences ($p < 0.05$) between experimental phases and capital letters indicate significant differences ($p < 0.05$) between olivine treatments within an experimental phase.

present in the guts after 96 h of depuration, suggesting a long gut passage time or possible reingestion of egested grains. Dissolved Ni concentrations remained stable (0.056–0.20 µmol L^{-1}, $N = 18$) throughout the depuration phase (Fig. 3C). Previous studies with *Gammarus* spp. have reported considerable variation in gut passage time from 0.5 h to more than 64 h depending on the ingested particle type (Straub et al., 2017; Willoughby and Earnshaw, 1982). Overall, the observed olivine egestion rate was within the range of egestion rates reported for other particle types in *Gammarus* spp. Cr concentrations in amphipods (Fig. 3B) and ASW (Fig. 3D) followed the same temporal trends as Ni concentrations, although lower accumulation was observed similar to the results of the acute exposure to different olivine grain sizes (Section 3.2).

3.3.2. Ingested olivine size distribution

Thousands of olivine grains of various sizes were ingested by *G. locusta* during the 96-h exposure experiment (Fig. 4B). Ingested olivine grains had a Feret diameter ranging from 0.1 to 185 µm and grains with a diameter between 0.3 and 8 µm were most abundant (89% of all particles) (Fig. 4A). The bulk olivine was comprised mostly (91%) of very small particles with a diameter between 0.3 and 1 µm, which were 64% less abundant in the guts of exposed amphipods (Fig. 4A). *G. locusta* mainly feeds on macroalgae and sediment detritus close to the seafloor in the lower intertidal and subtidal zone (Costa and Costa, 2000), which could explain the lower ingestion of very fine particles which would be suspended in the water column. Several microplastic exposure studies have also reported low ingestion rate of 1.0 to 1.6 µm (in diameter) particles in *Gammarus* spp. (Blarer and Burkhardt-Holm, 2016; Scherer et al., 2017). Overall, large amounts of small (mainly ≤10 µm) olivine particles were observed in the guts of exposed amphipods.

3.4. Chronic 3–99 µm olivine toxicity test

3.4.1. Survival rate

Chronic exposure to 3–99 µm olivine reduced median amphipod survival by half in the 100% w/w treatment (21%, $p < 0.001$) compared to the control (44%) (Fig. 5A). A significant negative relationship was observed between amphipod survival and whole body Ni concentrations ($\tau = -0.51$, $R^2 = 0.51$, $F(1, 22) = 23$, $p < 0.001$) (Fig. 5B), suggesting that metal-induced toxic effects involving oxidative damage (Fig. 10) and disruption of major cation homeostasis (Fig. 9) were likely the main reason for decreased amphipod survival in the 100% w/w treatment (Blewett and Leonard, 2017; DesMarias and Costa, 2019). A slightly higher median survival rate in the 1% w/w treatment (50%) compared to the control (44%) could be explained by stimulation of biological processes at low stress levels (i.e. hormesis), although the difference in survival rate was not statistically significant ($p = 0.92$) (Fig. 5A) (Rix et al., 2022).

Similar to our study, low control survival rates around 50% have been observed in other chronic laboratory experiments with *G. locusta* (Costa et al., 2005). This can be explained by cannibalism (Costa et al., 2005) and the relatively short maximum life span of around 16 weeks at 20 °C and 33‰ (Neuparth et al., 2002). Neuparth et al. (2002) reported an increase in amphipod life expectancy by at least 4 weeks at a temperature of 15 °C compared to 20 °C. However, for standardizing tests and reducing costs, Neuparth et al. (2002) recommended a temperature

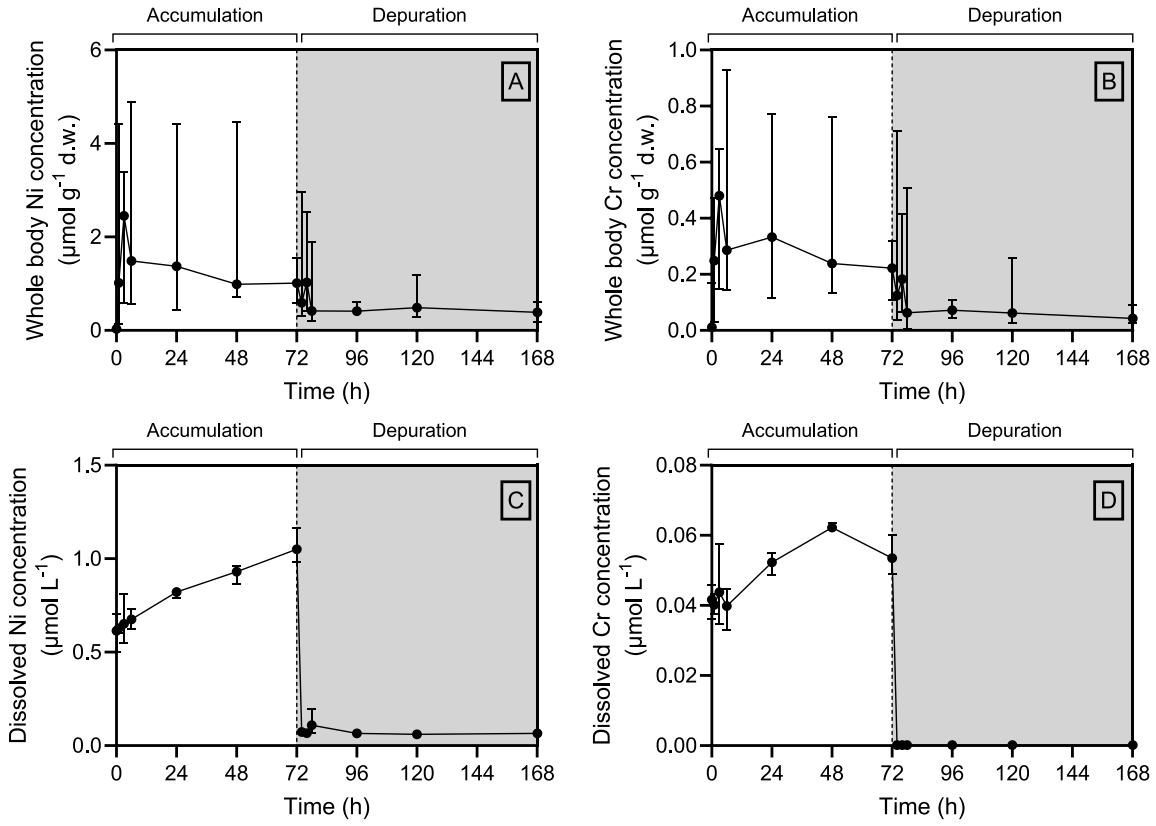

Fig. 3. Temporal evolution of nickel (Ni) and chromium (Cr) concentrations in amphipods (A, B) and artificial seawater (C, D) during 72 h pure olivine exposure (white area) and 96 h depuration (grey area). Median and range are shown for concentrations in amphipods ($N = 7$ or 8) and mean and range for concentrations in ASW ($N = 3$).

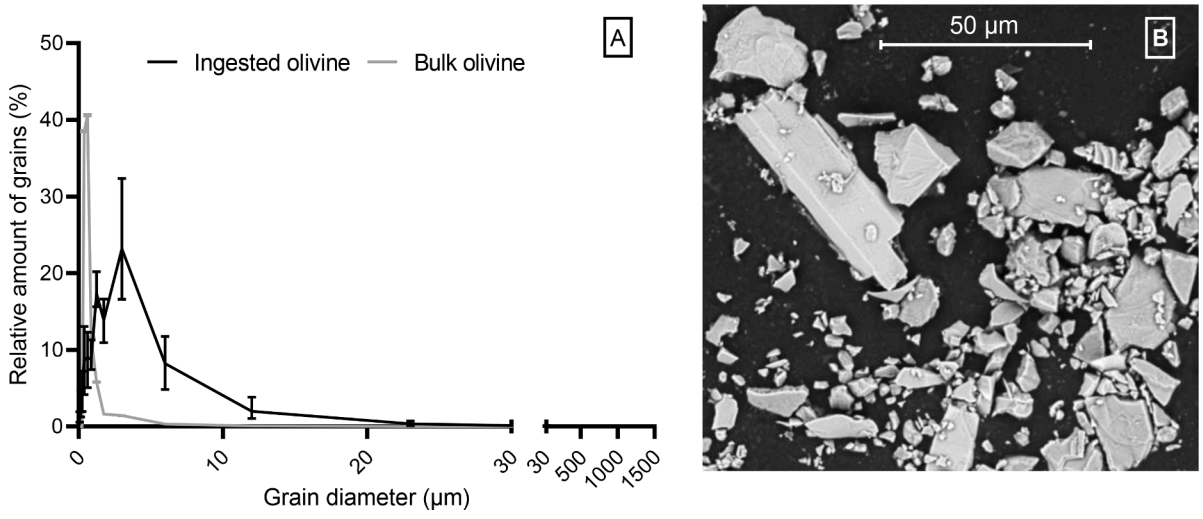

Fig. 4. Ingested olivine grains by *G. locusta*. (A) Number based particle size distribution for bulk 3–99 µm olivine (grey, $N = 4$) and ingested olivine in the guts of amphipods (black, $N = 9$ amphipods, 53206 particles measured) exposed for various times (2 – 72 h). The relative amount of grains (%) for different grain diameters (µm) is shown as median and range values. (B) Scanning electron microscope image of olivine grains present in the guts of an amphipod exposed to 3–99 µm olivine for 24 h.

of 20 °C for routine chronic sediment toxicity. Furthermore, 20 °C represents typical summer water temperatures in the Eastern Scheldt estuary (Rios-Yunes et al., 2023), which would likely coincide with the period of highest toxicological risk following olivine spreading. This is due to faster olivine dissolution and trace metal release during warmer temperatures (Rimstidt et al., 2012).

3.4.2. Individual growth

Surviving amphipods from the 25, 50, and 100% w/w olivine treatments were respectively 16 ($p = 0.013$), 27 ($p = 0.0015$) and 32% ($p < 0.001$) smaller (median ML: 6.6–8.1 mm) compared to control amphipods (median ML: 9.7 mm) (Fig. 6A). A difference in food availability cannot explain reduced growth, since sediment SOM

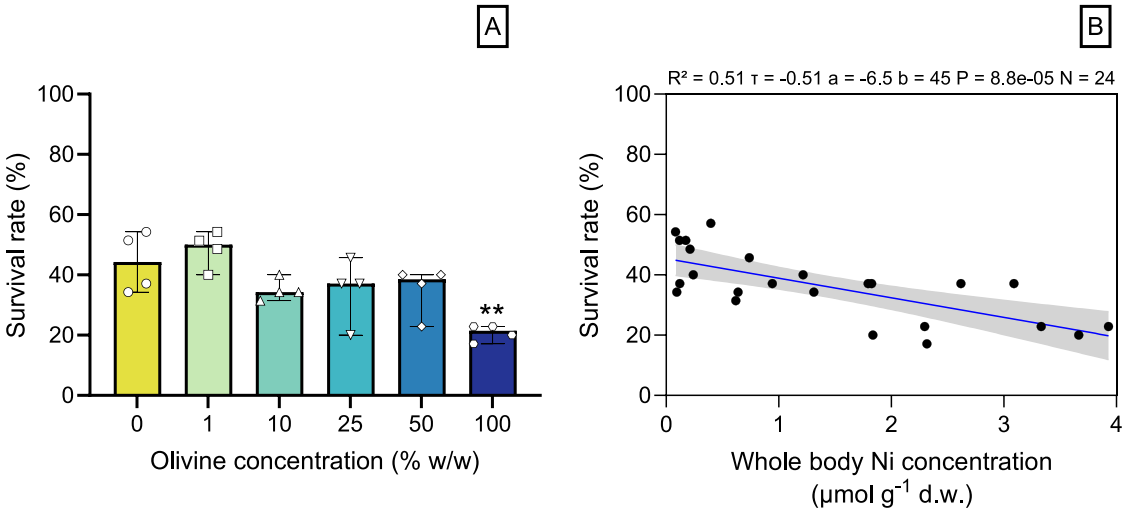

Fig. 5. (A) Survival rate (%) of *G. locusta* exposed to natural sediment mixed with various amounts of 3–99 µm olivine (expressed in % w/w) for 35 days. Median and range are shown (N = 4). Significance compared to 0% w/w olivine: * = $p < 0.05$, ** = $p < 0.01$, *** = $p < 0.001$. (B) Linear regression between *G. locusta* survival rate and whole body Ni concentration (µmol g^{-1} d.w.). Regression line (blue) with 95% confidence interval (dark grey shading) is shown. The coefficient of determination (R^2), Kendall correlation coefficient (τ), sample size (N), and regression line slope (a), intercept (b), and p value (P) are given.(For interpretation of the references to colour in this figure legend, the reader is referred to the web version of this article.)

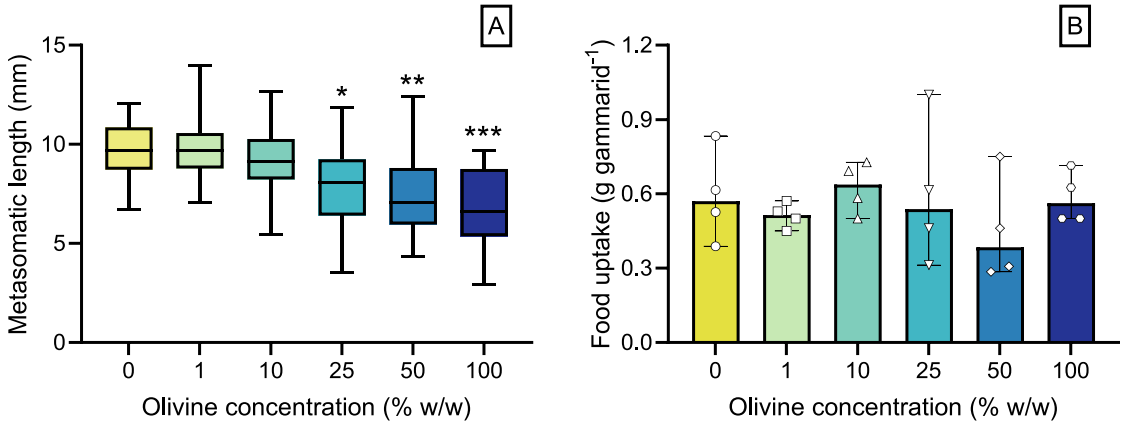

Fig. 6. (A) Box and whisker plots of the metasomatic length (mm) (N = 29–68 amphipods), and (B) bar plots of the food uptake (g $gammarid^{-1}$) (median and range, N = 4) for *G. locusta* exposed to natural sediment mixed with various amounts of 3–99 µm olivine (expressed in % w/w) for 35 days. Whiskers in (A) represent the minimum and maximum length. Significance compared to 0% w/w olivine: * = $p < 0.05$, ** = $p < 0.01$, *** = $p < 0.001$.

concentrations did not differ substantially among treatments (Table 1) and food (*Ulva* sp.) was provided *ad libitum*. Furthermore, limited stress is expected from differences in sediment grain size distribution among treatments, since *G. locusta* inhabits a wide range of sediment types and can tolerate exposure to sandy and silty sediments under laboratory conditions (Costa and Costa, 2000). Therefore, significant metal accumulation (Fig. 8A and B) likely resulted in oxidative stress (Fig. 10) and increased energy demand for detoxification and maintaining ion homeostasis which led to reduced individual growth (Brix et al., 2017). Amphipods did not compensate for reduced metabolic energy by increasing their feeding rate (Fig. 6B). In a natural ecosystem, a reduction in amphipod growth could have both population and community-level consequences via the reduction in reproductive output and lower food availability for higher trophic levels (e.g. fish and shorebirds), respectively (Sibley et al., 1997). Additionally, the important role of amphipods in nutrient recycling by detritus consumption and shaping of coastal landscapes through grazing on macroalgae could be compromised (Costa and Costa, 2000).

3.4.3. Reproductive traits

Chronic olivine exposure resulted in significant reproductive impairment in *G. locusta* at olivine concentrations of 10% w/w and higher (Fig. 7A–C). The median percentage of gravid females was significantly reduced from 100% in the control to 58 ($p = 0.048$), 33 ($p < 0.001$), and 20% ($p < 0.001$) in the 10, 50, and 100% w/w olivine treatments, respectively (Fig. 7A). Consequently, the median total number of embryos was only 8 (range: 0–35) in the 50% w/w ($p = 0.010$) and 5 (range: 0–35) in the 100% w/w ($p = 0.0090$) olivine treatment compared to a significantly higher 123 (range: 14–159) in the control (Fig. 7B). The median total number of juveniles was significantly reduced from 46 (range: 29–57) in the control to between 0 and 14 (median values) in treatments with olivine concentrations of 10% w/w and higher (Fig. 7C). From the significant negative relationship observed between reproductive endpoints and whole body Ni concentrations (Supplementary Figs. A.15A and A.16), we infer that metal toxicity was the driver for reproductive impairment in *G. locusta*.

Female *G. locusta* need to reach a size of approximately 7.5 to 8.3 mm (ML) to reproduce, and their brood size is positively correlated with body size (Neuparth et al., 2002). In our study, approximately 97% of

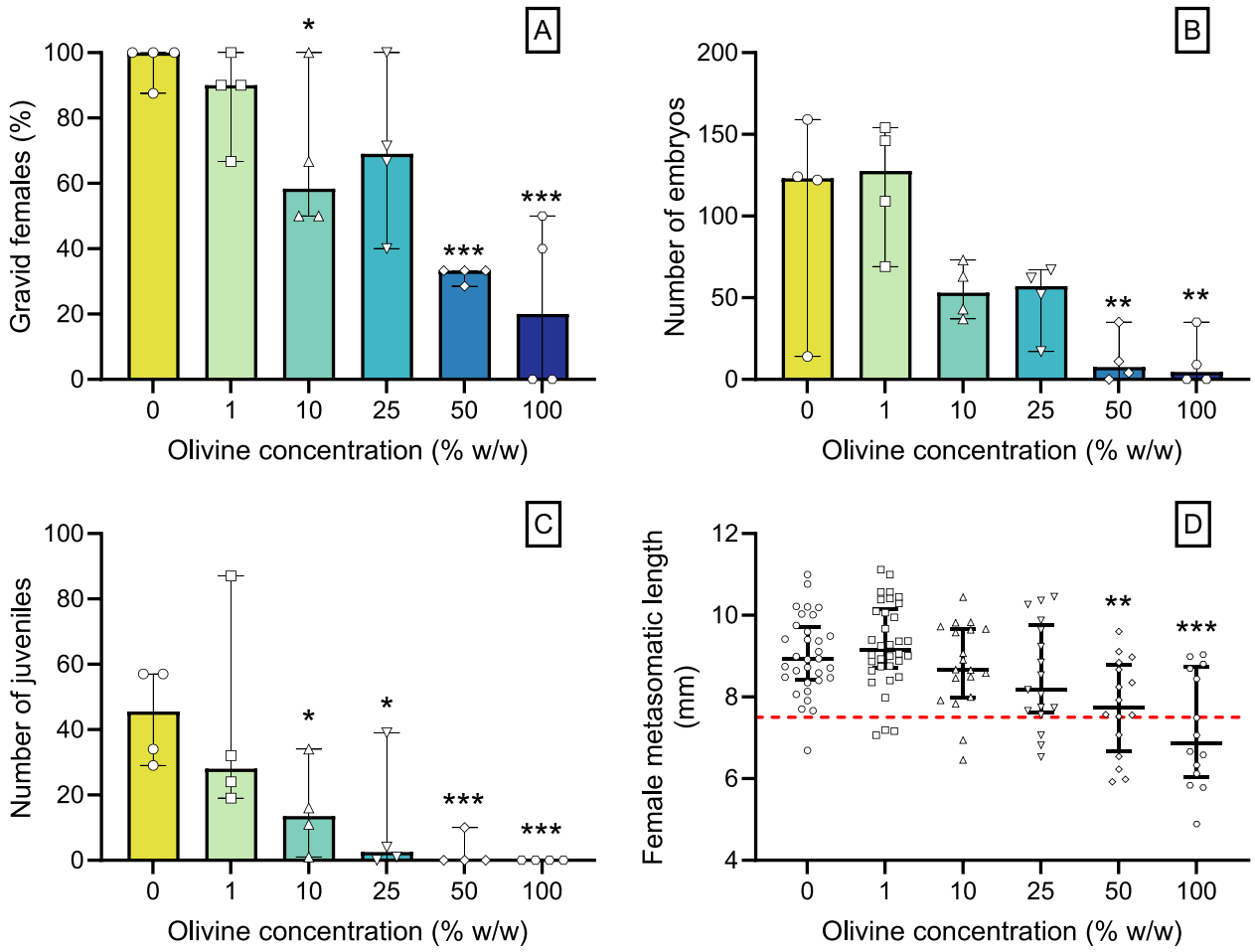

Fig. 7. (A) Percentage of gravid females, and total number of (B) embryos and (C) juveniles for *G. locusta* exposed to natural sediment mixed with various amounts of 3–99 μm olivine (expressed in % w/w) for 35 days. Median and range are shown ($N = 4$). (D) The metasomatic length of surviving females is shown as individual values, median, and IQR ($N = 14$–34 amphipods). Red dotted line in (D) represents the size of sexual maturity in *G. locusta* (7.5 mm) according to Neuparth et al. (2002). Significance compared to 0% w/w olivine: * = $p < 0.05$, ** = $p < 0.01$, *** = $p < 0.001$.(For interpretation of the references to colour in this figure legend, the reader is referred to the web version of this article.)

the surviving females in the control reached the estimated size of sexual maturity (>7.5 mm), while only 90, 82, 69, and 36% of the females in the 10, 25, 50, and 100% w/w olivine treatments reached this size (Fig. 7D). Hence, stunted growth can at least partly explain the lower percentage of gravid females in treatments with an olivine concentration of 10% w/w and higher. However, only 3.2% of the females larger than 7.5 mm were not gravid in the control while this was 29, 55, and 60% in the 10, 50, and 100% w/w olivine treatments. This can potentially be explained by increased brood abortion to preserve energy for individual fitness (Maltby and Naylor, 1990), or a reduction in pairing behaviour as a result of contaminant exposure (Love et al., 2020). Results for the number of embryos and juveniles per female are discussed in Supplementary Section SI 5.4.

3.4.4. Trace metal accumulation

Olivine-exposed amphipods showed significantly ($p < 0.001$) elevated whole body Ni (0.17–3.7 μmol g^{-1} d.w., $N = 24$) and Cr (0.049–0.65 μmol g^{-1} d.w., $N = 24$) concentrations compared to control amphipods (0.083–0.12 μmol Ni g^{-1} d.w. and 0.0059–0.017 μmol Cr g^{-1} d.w., $N = 4$) after 35 days of exposure (Fig. 8A and B). Whole body metal accumulation was dose dependent and Cr accumulation was generally lower than Ni accumulation, indicating lower Cr bioavailability (Fig. 8A and B). Amphipods were not depurated before analysis, so ingested olivine grains could have contributed significantly to the observed metal concentrations. However, since SOM concentrations in sediment (Table 1) and DOC concentrations in ASW (Supplementary Fig. A.8E) were low, higher trace metal bioavailability is expected (Blewett and Leonard, 2017).

Dissolved Ni concentrations were relatively stable in the control (0.034–0.24 μmol L^{-1}, $N = 30$) and increased dose dependently in the olivine treatments with concentrations up to 0.64 μmol L^{-1} in the 50% w/w and 100% w/w treatment (Fig. 8C). Dissolved Cr concentrations (<0.39–51 nmol L^{-1}, $N = 180$) did not differ significantly among treatments or sampling days (Fig. 8D). However, measured dissolved Ni and Cr concentrations were significantly elevated compared to typical concentrations (<10 nmol L^{-1}) for coastal waters (Flipkens et al., 2021). Nevertheless, observed dissolved Ni concentrations could potentially be reached under realistic 1 to 10% w/w coastal 3–99 μm olivine applications in shallow (10 m water depth) temperate (15 °C) coastal seas with a water residence time of more than one month (Supplementary Section SI 5.3) and thus represent possibly realistic exposure concentrations for *G. locusta*.

3.4.5. Whole body major cation content

Chronic exposure to 100% w/w olivine resulted in a significant 16 to 21% reduction of whole body Ca, Na, and K concentrations compared to the control (Fig. 9A–C). Whole body Mg concentrations were significantly elevated in amphipods exposed to olivine concentrations of 25% w/w and higher, likely as a result of olivine ingestion (Fig. 9D). Disruption of Ca, Mg, Na, and K ionoregulation has been previously

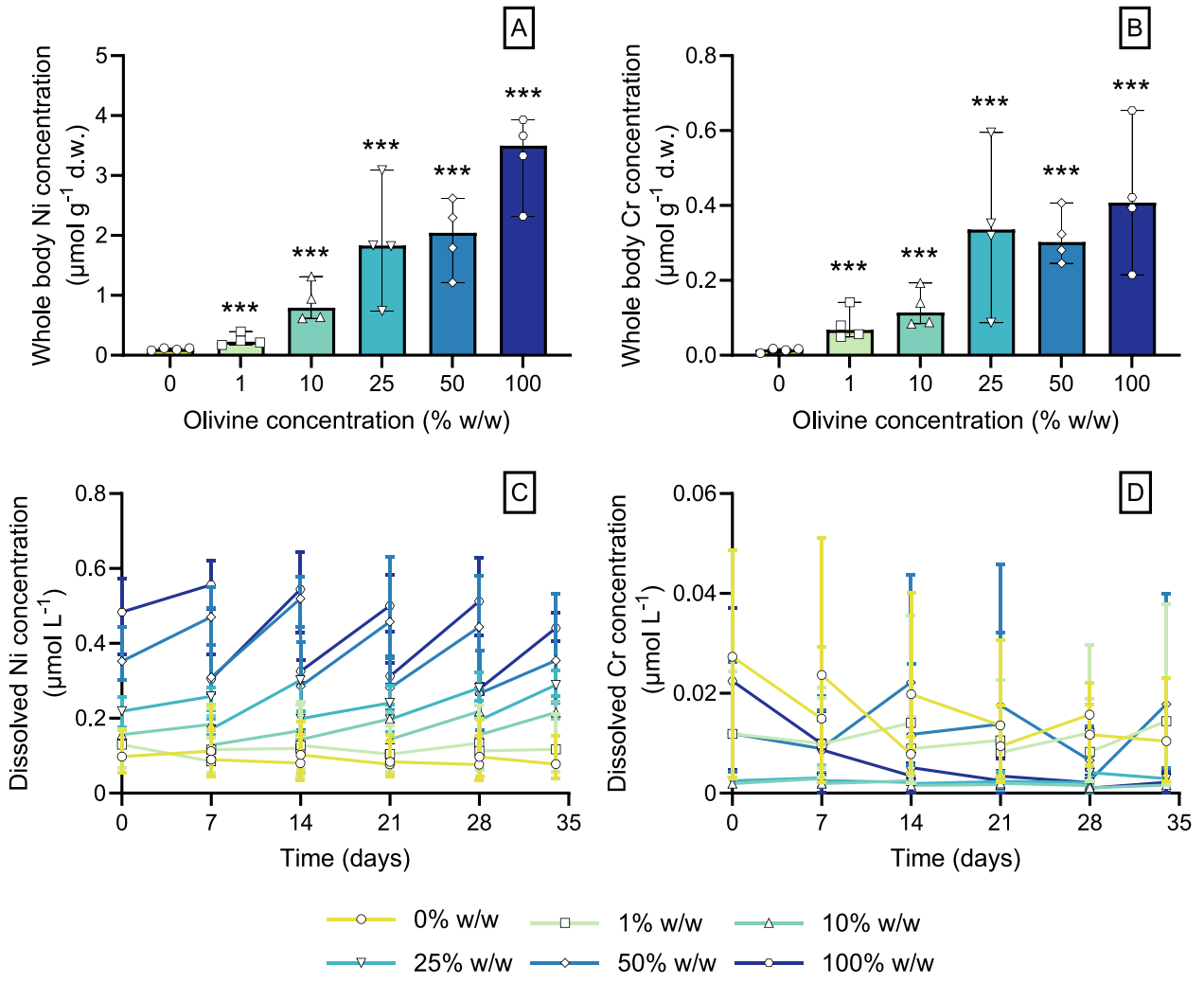

Fig. 8. Whole body concentration (µmol g^{-1} dry weight) of (A) nickel (Ni), and (B) chromium (Cr) in pooled *G. locusta* exposed to natural sediment mixed with various amounts of 3–99 µm olivine (expressed in % w/w) for 35 days. Median and range are shown ($N = 4$). Significance compared to 0% w/w olivine: * = $p < 0.05$, ** = $p < 0.01$, *** = $p < 0.001$. Temporal evolution of dissolved (C) Ni and (D) Cr concentrations (µmol L^{-1}) in artificial seawater during the 35 day experiment. Mean and range ($N = 2$ or 3) are shown.

observed in marine invertebrates exposed to Ni concentrations ranging from 0.14 to 51 µmol L^{-1} via ion mimicry and inhibition of ion transporters such as the Ca^{2+}- and Na^{+}/K^{+}-ATPases (Blewett and Leonard, 2017; Brix et al., 2017). Furthermore, both Ni and Cr can induce oxidative stress, which can cause oxidative degradation of cell membranes (Section 3.4.6.) and thus disrupt the activity of transmembrane ion transporters (Lushchak, 2011). Therefore, disruption of ion homeostasis is likely the result of Ni and Cr toxicity in amphipods exposed to 100% w/w olivine.

3.4.6. Lipid peroxidation

TBARS concentrations were approximately 1.5 times higher in the 10% w/w olivine treatment (median = 1.08 µmol g^{-1} w.w.) and doubled in the 100% w/w treatment (1.54 µmol g^{-1} w.w.) compared to the control (median = 0.74 µmol g^{-1} w.w.) (Fig. 10A). A significant positive relationship ($\tau = 0.69$, $R^2 = 0.71$, $F(1, 11) = 27$, $p < 0.001$) was observed between TBARS concentrations and whole body Ni concentrations (Fig. 10B), suggesting metal-induced oxidative damage.

Nickel could cause oxidative stress by substituting for Fe^{2+} in the reactive oxygen species (ROS) producing Fenton/Haber Weiss reactions, inhibiting antioxidant enzyme activity such as catalase, or by decreasing the ROS scavenging potential of compounds like glutathione by complex formation (Blewett and Leonard, 2017; Brix et al., 2017). In previous studies, significant changes in antioxidant enzyme activities and MDA levels have been observed in *Tigriopus japonicus* and *Mytilus galloprovincialis* exposed to Ni concentrations of 2.1 and 13 µmol L^{-1} during a 12 and 4-day exposure, respectively (Attig et al., 2014; Wang and Wang, 2010). Additionally, Cr(VI) exposure resulted in lipid peroxidation at concentrations as low as 0.019 µmol L^{-1} in gills of *Venus verrucosa* exposed for 7 days (Chaâbane et al., 2020). Reduction of Cr(VI) to Cr(III) after cellular uptake is accompanied by significant ROS production resulting in oxidative stress if antioxidant responses are inadequate (DesMarias and Costa, 2019). Although Cr is present as less toxic Cr(III) in chromite associated with dunite, release and oxidation of chromite nanoparticles could result in elevated Cr(VI) exposure, accumulation and potential toxicity (Das et al., 2021; Flipkens et al., 2021). Overall, olivine exposure resulted in oxidative stress, likely as a result of significant Ni and Cr accumulation (Fig. 8A and B).

3.4.7. Implications for coastal enhanced olivine weathering

Olivine exposure effects on aquatic biota remain scarcely studied (Hutchins et al., 2023; Ren et al., 2021; Xie et al., 2023), preventing accurate assessment of the environmentally safe CDR scale of coastal enhanced olivine weathering. An increase in the abundance of biofilm forming particle attached microbes was observed 10 days after 1% w/w olivine addition to natural seawater (Ren et al., 2021). Furthermore, Mg

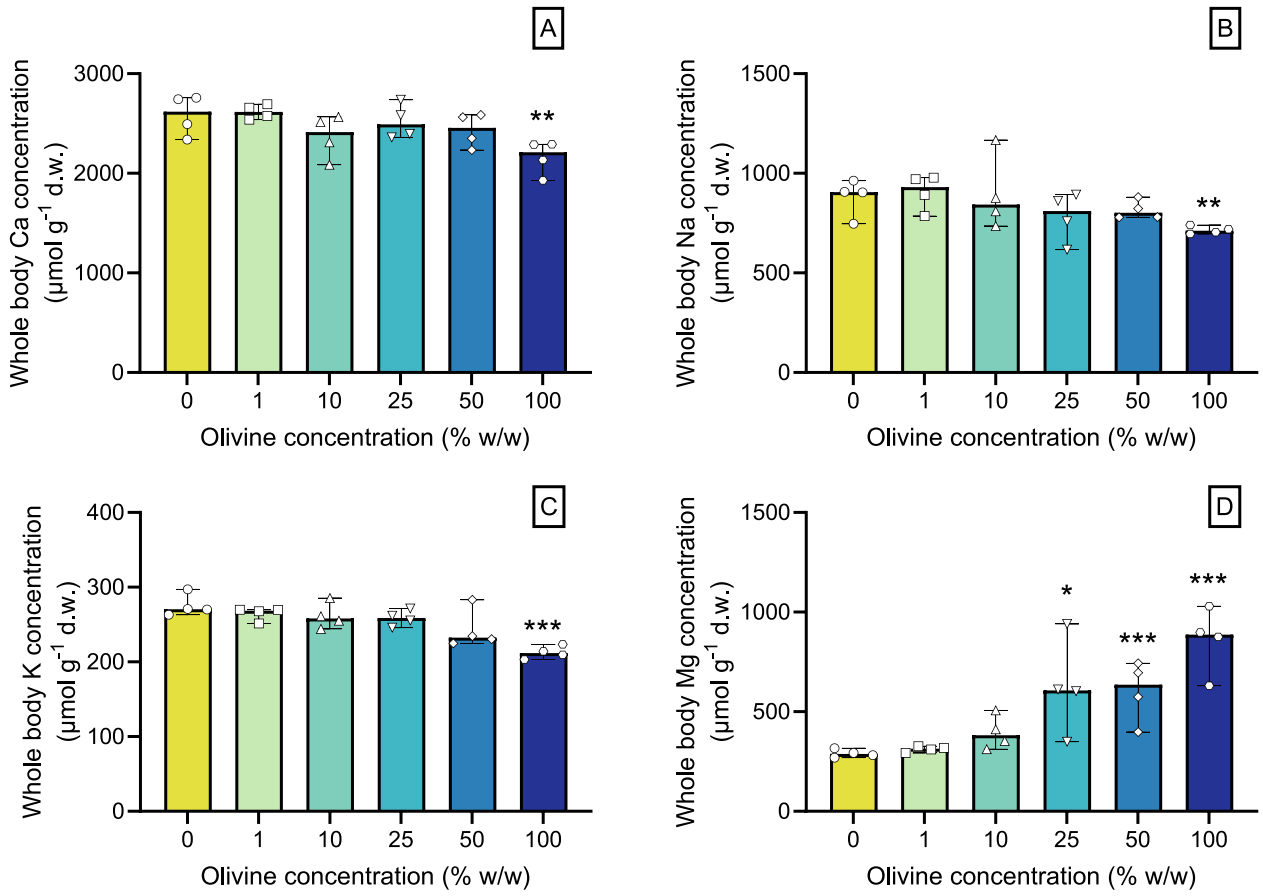

Fig. 9. Whole body concentration (µmol g^{-1} dry weight) of (A) calcium (Ca), (B) sodium (Na), (C) potassium (K), and (D) magnesium (Mg) in pooled *G. locusta* exposed to natural sediment mixed with various amounts of 3–99 µm olivine (expressed in % w/w) for 35 days. Median and range are shown ($N = 4$). Significance compared to 0% w/w olivine: * = $p < 0.05$, ** = $p < 0.01$, *** = $p < 0.001$.

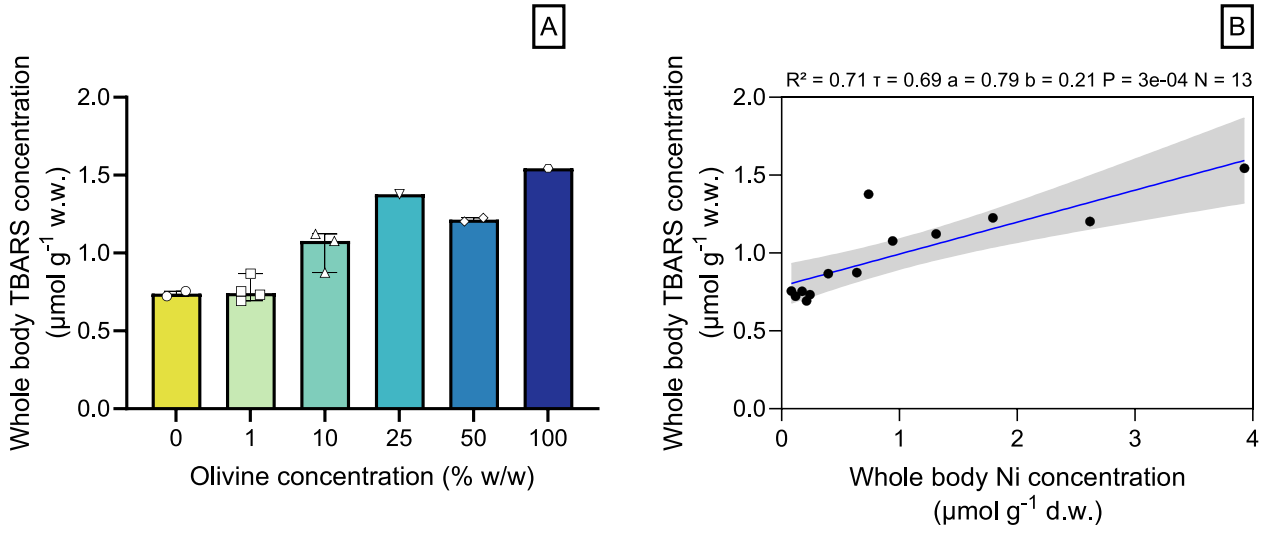

Fig. 10. (A) Whole body thiobarbituric acid reactive substances (TBARS) concentration (µmol g^{-1} w.w.) in pooled *G. locusta* exposed to natural sediment mixed with various amounts of 3–99 µm olivine (expressed in % w/w) for 35 days. Median and range are shown ($N = 4$). Significance compared to 0% w/w olivine: * = $p < 0.05$, ** = $p < 0.01$, *** = $p < 0.001$. (B) Linear regression between whole body TBARS concentration and whole body Ni concentration (µmol g^{-1} d.w.) in pooled *G. locusta*. Regression line (blue) with 95% confidence interval (dark grey shading) is shown. The coefficient of determination (R^2), Kendall correlation coefficient (τ), sample size (N), and regression line slope (a), intercept (b), and p value (P) are given.(For interpretation of the references to colour in this figure legend, the reader is referred to the web version of this article.)

release from olivine dissolution promoted the growth of the freshwater green microalgae *Chlamydomonas reinhardtii* and *Chlorella pyrenoedosa* during a 9 day exposure 8 g of olivine L^{-1} (Xie et al., 2023). Finally, positive and neutral growth responses were observed for two marine diatom species, one marine coccolithophore, and three marine cyanobacteria grown in synthetic olivine leachates with Ni(II) and Cr(VI) concentrations up to 0.13 and 0.12 μmol L^{-1} for a maximum of 10 days (Hutchins et al., 2023).

In contrast to the overall neutral to positive effects of olivine exposure reported by previous studies, we observed reduced survival, growth, and reproduction of *G. locusta* chronically exposed to fine-grained olivine. The percentage of gravid females and juvenile production were significantly reduced at 10% w/w olivine and higher after 35 days of exposure (Fig. 7A and C), resulting in a highest no observed effect concentration (NOEC) for 1% w/w olivine. Additionally, a 10% effect concentrations (EC10) of 0.99% (0–4.4%) w/w olivine for juvenile production and 5.5% (0–17%) w/w olivine for percentage of gravid females were obtained (Supplementary Section SI 5.7). In regards to chemical risk assessment, an arbitrary assessment factor of 100 would be applied to the lowest NOEC or EC10 value when only one chronic marine sediment toxicity test was conducted, resulting in a predicted no effect concentration (PNEC) of 0.01% w/w olivine (ECHA, 2008). This PNEC value is very low, even compared to the conservative olivine application guideline of 0.059–1.4 kg olivine m^{-2} or 0.056 to 1.3% w/w derived by Flipkens et al. (2021) based on existing Ni sediment quality guidelines. Hence, these findings highlight the need for additional olivine toxicity data for a range of marine species to derive accurate olivine PNEC values. Moreover, molecular endpoints (e.g. antioxidant enzyme expression and activity levels) should be considered in future olivine toxicity tests to advance the understanding of molecular mechanisms that drive Ni and Cr toxicity in marine biota. Furthermore, the effect of grain size on olivine toxicity should also be explored, since larger grains might be less toxic because they lead to lower metal bioaccumulation (Fig. 2A and B). Finally, research on the environmental safety of alternative silicates with a lower trace metal content compared to dunite, such as basalt, kimberlite, or wollastonite for use in coastal enhanced weathering seems advised.

4. Conclusions

Coastal enhanced olivine weathering is a proposed atmospheric CO_2 removal strategy for climate change mitigation. However, uncertainties regarding the CO_2 sequestration potential and environmental safety prevent fast upscaling of the technique from laboratory studies to field trials. This study investigated acute 24 to 96 h bioaccumulation and chronic 35-day bioaccumulation and toxicity of olivine in the marine amphipod *G. locusta*. Acute olivine exposure resulted in significant grain size dependent olivine ingestion as well as whole body and tissue trace metal accumulation in *G. locusta*. The tissue bioaccumulation of Ni was 3 to 8 times higher compared to Cr, and limited Cr accumulation was observed in the seawater dissolved phase, suggesting lower Cr bioavailability. Thousands of small olivine grains (mainly 0.3 to 8 μm in size) were observed in the guts of exposed amphipods, but further experimental evidence is needed to assess their significance as a trace metal exposure pathway. Chronic 35-day exposure of juvenile amphipods to 3–99 μm olivine resulted in significant adverse effects on survival, growth, and reproduction, likely as a result of metal induced oxidative stress and disruption of Ca^{2+}, Na^{+}, and K^{+} homeostasis. The total juvenile production and percentage of gravid females was significantly reduced at an exposure concentration of 10% w/w olivine. From this first sediment olivine toxicity test, application of arbitrary risk assessment protocols yields a very low PNEC of 0.01% w/w olivine (3–99 μm), highlighting the need for additional marine olivine toxicity data to strengthen the derived olivine application guideline. Furthermore, the CO_2 sequestration potential and ecosystem effects of silicates with a lower Ni and Cr content (e.g. basalt, kimberlite, and wollastonite) should be investigated to assess the scale at which these rocks could be safely used for coastal enhanced silicate weathering.

Appendix A. Supplementary material

Gammarus species, sex, and size determination details, sediment and olivine geochemical properties, and additional results from the different olivine exposure experiments with *G. locusta* can be found in the Supplementary Word file. Research data is accessible through the Marine Data Archive at https://doi.org/10.14284/614.

CRediT authorship contribution statement

Gunter Flipkens: Conceptualization, Data curation, Formal analysis, Investigation, Methodology, Visualization, Writing – original draft, Writing – review & editing. **Katharina Horoba:** Conceptualization, Formal analysis, Investigation, Methodology. **Kobe Bostyn:** Formal analysis, Investigation. **Luna J.J. Geerts:** Formal analysis, Writing – review & editing. **Raewyn M. Town:** Conceptualization, Methodology, Supervision, Writing – review & editing. **Ronny Blust:** Conceptualization, Methodology, Funding acquisition, Supervision, Writing – review & editing.

Declaration of Competing Interest

The authors declare that they have no known competing financial interests or personal relationships that could have appeared to influence the work reported in this paper.

Data availability

Research data is accessible through the Marine Data Archive at https://doi.org/10.14284/614.

Acknowledgements

The authors thank Karin Van den Bergh for conducting the DOC analysis. Furthermore, Kayawe Valentine Mubiana and Steven Joosen are thanked for their help with the element analysis. We also appreciate the assistance of Jenevieve Hara with the ingested particle size analysis and the help of Laura Pattyn with the amphipod and sediment collection. This work was supported by the Fonds voor Wetenschappelijk Onderzoek-Vlaanderen (FWO) [grant number S000619N].

Supplementary materials

Supplementary material associated with this article can be found, in the online version, at doi:10.1016/j.aquatox.2023.106662.

References

Attig, H., Kamel, N., Sforzini, S., Dagnino, A., Jamel, J., Boussetta, H., Viarengo, A., Banni, M., 2014. Effects of thermal stress and nickel exposure on biomarkers responses in *Mytilus galloprovincialis* (Lam). Mar. Environ. Res. 94, 65–71. 10.1016/j.marenvres.2013.12.006.

Bach, L.T., Gill, S.J., Rickaby, R.E., Gore, S., Renforth, P., 2019. CO_2 removal with enhanced weathering and ocean alkalinity enhancement: potential risks and co-benefits for marine pelagic ecosystems. Front. Clim. 1, 7. https://doi.org/10.3389/fclim.2019.00007.

Blarer, P., Burkhardt-Holm, P., 2016. Microplastics affect assimilation efficiency in the freshwater amphipod *Gammarus fossarum*. Environ. Sci. Pollut. Res. 23, 23522–23532. https://doi.org/10.1007/s11356-016-7584-2.

Blewett, T.A., Leonard, E.M., 2017. Mechanisms of nickel toxicity to fish and invertebrates in marine and estuarine waters. Environ. Pollut. 223, 311–322. https://doi.org/10.1016/j.envpol.2017.01.028.

Brix, K.V., Schlekat, C.E., Garman, E.R., 2017. The mechanisms of nickel toxicity in aquatic environments: an adverse outcome pathway analysis. Environ. Toxicol. Chem. 36 (5), 1128–1137. https://doi.org/10.1002/etc.3706.

Caserini, S., Storni, N., Grosso, M., 2022. The availability of limestone and other raw materials for ocean alkalinity enhancement. Glob. Biogeochem. Cycles. 36 (5), e2021GB007246 https://doi.org/10.1029/2021GB007246.
CEM Corporation, 1999. Chromite Ore Microwave Sample Preparation Note: 5OS-47. http://www.uwm.edu.pl/kchemsr/MARS/OXIDSUL/Chromit.pdf (accessed 04/07/2022).
Chaâbane, M., Bejaoui, S., Trabelsi, W., Telahigue, K., Chetoui, I., Chalghaf, M., Zeghal, N., Soudani, N., 2020. The potential toxic effects of hexavalent chromium on oxidative stress biomarkers and fatty acids profile in soft tissues of *Venus verrucosa*. Ecotoxicol. Environ. Saf. 196, 110562 https://doi.org/10.1016/j.ecoenv.2020.110562.
Chakraborty, P., Sarkar, A., Vudamala, K., Naik, R., Nath, B.N., 2015. Organic matter—A key factor in controlling mercury distribution in estuarine sediment. Mar. Chem. 173, 302–309. https://doi.org/10.1016/j.marchem.2014.10.005.
Costa, F., Costa, M., 2000. Review of the ecology of *Gammarus locusta* [L.]. Pol. Arch. Hydrobiol. 47 (3–4), 541–559.
Costa, F.O., Neuparth, T., Correia, A.D., Costa, M.H., 2005. Multi-level assessment of chronic toxicity of estuarine sediments with the amphipod *Gammarus locusta*: II. Organism and population-level endpoints. Mar. Environ. Res. 60 (1), 93–110. https://doi.org/10.1016/j.marenvres.2004.08.005.
Das, P.K., Das, B.P., Dash, P., 2021. Chromite mining pollution, environmental impact, toxicity and phytoremediation: a review. Environ. Chem. Lett. 19 (2), 1369–1381. https://doi.org/10.1007/s10311-020-01102-w.
den Otter, J., Pröfrock, D., Bünning, T., Strehse, J., van der Heijden, A., Maser, E., 2023. Release of ammunition-related compounds from a Dutch marine dump site. Toxics 11 (3), 238.
DesMarias, T.L., Costa, M., 2019. Mechanisms of chromium-induced toxicity. Curr. Opin. Toxicol. 14, 1–7. https://doi.org/10.1016/j.cotox.2019.05.003.
Dickson, A.G., Sabine, C.L., Christian, J.R., 2007. Guide to Best Practices for Ocean CO_2 Measurements, North Pacific Marine Science Organization, 193. PICES Special Publication, Sidney, British Columbia, p. 191. IOCCP Report 198.
Duan, L., Song, J., Li, X., Yuan, H., Zhuang, W., 2022. Potential risks of CO_2 removal project based on carbonate pump to marine ecosystem. Sci. Total Environ., 160728 https://doi.org/10.1016/j.scitotenv.2022.160728.
ECHA, 2008. Guidance on information requirements and chemical safety assessment Chapter R.10: Characterisation of dose [concentration]-response for environment. https://echa.europa.eu/documents/10162/13632/information_requirements_r10_en.pdf/bb902be7-a503-4ab7-9036-d866b8ddce69 (accessed 8 March 2023).
Flipkens, G., Blust, R., Town, R.M., 2021. Deriving nickel (Ni (II)) and chromium (Cr (III)) based environmentally safe olivine guidelines for coastal enhanced silicate weathering. Environ. Sci. Technol. 55 (18), 12362–12371. https://doi.org/10.1021/acs.est.1c02974.
Heiri, O., Lotter, A.F., Lemcke, G., 2001. Loss on ignition as a method for estimating organic and carbonate content in sediments: reproducibility and comparability of results. J. Paleolimnol. 25 (1), 101–110. https://doi.org/10.1023/A:1008119611481.
Hutchins, D.A., Fu, F.-X., Yang, S.-C., John, S.G., Romaniello, S.J., Andrews, M.G., Walworth, N.G., 2023. Responses of keystone phytoplankton groups to olivine dissolution products and implications for carbon dioxide removal via ocean alkalinity enhancement. bioRxiv. https://doi.org/10.1101/2023.04.08.536121.
Love, A.C., Crooks, N., Ford, A.T., 2020. The effects of wastewater effluent on multiple behaviours in the amphipod, *Gammarus pulex*. Environ. Pollut. 267, 115386 https://doi.org/10.1016/j.envpol.2020.115386.
Lushchak, V.I., 2011. Environmentally induced oxidative stress in aquatic animals. Aquat. Toxicol. 101 (1), 13–30. https://doi.org/10.1016/j.aquatox.2010.10.006.
Maltby, L., Naylor, C., 1990. Preliminary observations on the ecological relevance of the Gammarusscope for growth'assay: effect of zinc on reproduction. Funct. Ecol. 393–397. https://doi.org/10.2307/2389601.
Meysman, F.J., Montserrat, F., 2017. Negative CO_2 emissions via enhanced silicate weathering in coastal environments. Biol. Lett. 13 (4), 20160905.
Minx, J.C., Lamb, W.F., Callaghan, M.W., Fuss, S., Hilaire, J., Creutzig, F., Amann, T., Beringer, T., de Oliveira Garcia, W., Hartmann, J., 2018. Negative emissions—Part 1: research landscape and synthesis. Environ. Res. Lett. 13 (6), 063001 https://doi.org/10.1088/1748-9326/aabf9b.
Neuparth, T., Correia, A.D., Costa, F.O., Lima, G., Costa, M.H., 2005. Multi-level assessment of chronic toxicity of estuarine sediments with the amphipod *Gammarus locusta*: I. Biochemical endpoints. Mar. Environ. Res. 60 (1), 69–91. https://doi.org/10.1016/j.marenvres.2004.08.006.
Neuparth, T., Costa, F.O., Costa, M.H., 2002. Effects of temperature and salinity on life history of the marine amphipod *Gammarus locusta*. Implications for ecotoxicological testing. Ecotoxicology 11 (1), 61–73. https://doi.org/10.1023/A:1013797130740.
Ouyang, Y., Zhang, J., Ou, L.T., 2006. Temporal and spatial distributions of sediment total organic carbon in an estuary river. J. Environ. Qual. 35 (1), 93–100. https://doi.org/10.2134/jeq2005.0221.
Ren, H., Hu, Y., Liu, J., Zhang, Z., Mou, L., Pan, Y., Zheng, Q., Li, G., Jiao, N., 2021. Response of a coastal microbial community to olivine addition in the Muping Marine Ranch, Yantai. Front. Microbiol. 12, 805361 https://doi.org/10.3389/fmicb.2021.805361.
Rimstidt, J.D., Brantley, S.L., Olsen, A.A., 2012. Systematic review of forsterite dissolution rate data. Geochim. Cosmochim. Acta. 99, 159–178. https://doi.org/10.1016/j.gca.2012.09.019.
Rios-Yunes, D., Tiano, J.C., van Rijswijk, P., De Borger, E., van Oevelen, D., Soetaert, K., 2023. Long-term changes in ecosystem functioning of a coastal bay expected from a shifting balance between intertidal and subtidal habitats. Cont. Shelf Res. 254, 104904.
Rix, R.R., Guedes, R.N.C., Cutler, G.C., 2022. Hormesis dose–response contaminant-induced hormesis in animals. Curr. Opin. Toxicol. 30, 100336.
Scherer, C., Brennholt, N., Reifferscheid, G., Wagner, M., 2017. Feeding type and development drive the ingestion of microplastics by freshwater invertebrates. Sci. Rep. 7 (1), 17006. https://doi.org/10.1038/s41598-017-17191-7.
Schlacher, T.A., Noriega, R., Jones, A., Dye, T., 2012. The effects of beach nourishment on benthic invertebrates in eastern Australia: impacts and variable recovery. Sci. Total Environ. 435, 411–417. https://doi.org/10.1016/j.scitotenv.2012.06.071.
Sibley, P.K., Benoit, D.A., Ankley, G.T., 1997. The significance of growth in Chironomus tentans sediment toxicity tests: relationship to reproduction and demographic endpoints. Environ. Toxicol. Chem. 16 (2), 336–345. https://doi.org/10.1002/etc.5620160232.
Straub, S., Hirsch, P.E., Burkhardt-Holm, P., 2017. Biodegradable and petroleum-based microplastics do not differ in their ingestion and excretion but in their biological effects in a freshwater invertebrate *Gammarus fossarum*. Int. J. Environ. Res. Public Health. 14 (7), 774. https://doi.org/10.3390/ijerph14070774.
Wang, M., Wang, G., 2010. Oxidative damage effects in the copepod *Tigriopus japonicus* Mori experimentally exposed to nickel. Ecotoxicology 19, 273–284. https://doi.org/10.1007/s10646-009-0410-6.
Wang, W.-X., Griscom, S.B., Fisher, N.S., 1997. Bioavailability of Cr (III) and Cr (VI) to marine mussels from solute and particulate pathways. Environ. Sci. Technol. 31 (2), 603–611. https://doi.org/10.1021/es960574x.
Willoughby, L., Earnshaw, R., 1982. Gut passage times in *Gammarus pulex* (Crustacea, Amphipoda) and aspects of summer feeding in a stony stream. Hydrobiologia 97, 105–117. https://doi.org/10.1007/BF00011964.
Xie, T., Zhao, L., Wu, Y., 2023. Peridotite dissolution in the presence of green microalgae: implications for a geoengineering strategy of CO_2 sequestration. J. Asian Earth Sci. 241, 105486.